Performance of Industrial Residues as Low Cost Oxygen Carriers

Citation for the original published paper (version of record):
Xu, L., Schwebel, G., Knutsson, P. et al (2017). Performance of Industrial Residues as Low Cost Oxygen Carriers. Energy Procedia, 114: 361-370. http://dx.doi.org/10.1016/j.egypro.2017.03.1178

Available online at www.sciencedirect.com

ScienceDirect

Energy Procedia 114 (2017) 361 – 370

Energy Procedia

13th International Conference on Greenhouse Gas Control Technologies, GHGT-13, 14-18 November 2016, Lausanne, Switzerland

Performance of industrial residues as low cost oxygen carriers

Lei Xu[a], Georg L. Schwebel[b], Pavleta Knutsson[c], Henrik Leion[c]*, Zhenshan Li[a], Ningsheng Cai[a]

[a]*Key Laboratory for Thermal Science and Power Engineering of Ministry of Education, Beijing Municipal Key Laboratory for CO2 Utilization & Reduction, Department of Thermal Engineering, Tsinghua University, Beijing 100084, China*
[b]*Department of Energy and Environment, Chalmers University of Technology, S-412 96 Göteborg, Sweden*
[c]*Department of Environmental Inorganic Chemistry, Chalmers University of Technology, S-412 96 Göteborg, Sweden*

Abstract

In Chemical-looping combustion (CLC) an oxygen carrier is circulating, and transporting oxygen, between an air and fuel reactor, thus separating the flue gas stream from the nitrogen in the air. Except for the oxygen carrier all parts of a CLC system are conventional fluidized bed technology. Here, four iron-based industrial residues, and the conventional oxygen carrier ilmenite, are examined as oxygen carrier. The results indicate that two of the material, exhibit a better performance than ilmenite. This opens the possibility of not using virgin material as oxygen carrier and offers a new possible use for industrial residue material.

Peer-review under responsibility of the organizing committee of GHGT-13.

Keywords: Chemical-looping combustion (CLC); oxygen carrier; industrial residue material

1. Introduction

Chemical-looping combustion (CLC) is a promising technology for burning fossil fuels with inherent CO_2 capture [1]. The general chemical-looping principle is shown in Fig. 1. CLC is generally carried out in two reaction steps. The fuel is used to reduce a solid oxygen carrier, typically a metal oxide, a reaction referred to as reduction. The reduced oxygen carrier is then reoxidized by air in a separate reaction step, thus referred to as oxidation. These two steps are commonly carried out in two separate reactors, the fuel reactor and the air reactor, with oxygen carrier's circulating

* Corresponding author. Tel.: +46-31-7722818; fax: +46-31-7722853.
E-mail address: Leion@chalmers.se

Peer-review under responsibility of the organizing committee of GHGT-13.
doi:10.1016/j.egypro.2017.03.1178

between them. The gases from both reactors never mix and a stream of H_2O and CO_2 is obtained at the outlet of the fuel reactor which inherently stays separated from the air nitrogen.

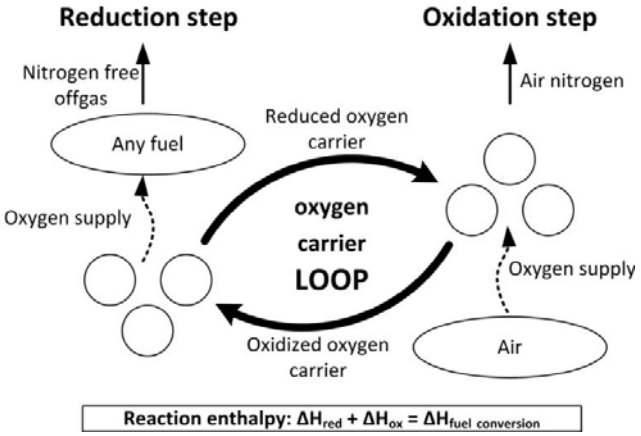

Fig. 1. Chemical-looping principle for thermochemical fuel conversion [2].

The oxidation of the reduced oxygen carrier in the air reactor is exothermic, whereas the reaction in the fuel reactor can be either exothermic or endothermic, depending on the choice of fuel and oxygen carrier. Overall the amount of heat produced is the same as for conventional combustion.

The principle of using solid oxygen carrier material to provide oxygen for thermochemical fuel conversion was proposed in the 1940s [3] to reform methane. The idea of CLC was patented as process for CO_2 production from carbonaceous sources in the 50s [4]. The same principle was proposed later on with the goal to lower the irreversibility of combustion [5, 6]. With the increasing recognition of anthropogenic climate change, the concept was investigated to recover CO_2 from the exhaust of combustion systems for power generation [7, 8]. Since then, obtaining CO_2 capture with low energy penalty for power sector is the main driving force for the CLC research.

Gaseous fuels [9-11], such as natural gas or syngas, and solid fuels [12-18], such as coal or biomass, have been widely investigated in the literature as possible fuels in CLC. While the application of gaseous fuels appears to be less problematic, for solid fuels, losses of oxygen carriers due to possible side reaction with ash [19], as well as material withdrawn from the reactor with the ash, may lead to high expected amounts of oxygen carrier makeup [18]. This increases the demand for abundant, low cost and environmental friendly oxygen carrier materials [14]. Possible materials under investigation have been natural ores [20-24] and industrial residues or by-products [25-28]. Among the natural ores, ilmenite has been most widely investigated [21, 29-32]. Five kinds of ilmenite from different resources was compared (Norway, Canada, South Africa and Madagascar) [23] and the reactivity of the Norwegian ilmenite was higher than the others. It was found that the reactivity of fresh materials increases with successive redox cycles. This is referred to as activation [33].

Apart from using ores and industrial residues in CLC solely for the purpose of electric power generation, CLC with these materials could also be integrated into other industrial processes The extractive industry, as well as the steel industry, generates large CO_2 emissions. If one could find promising oxygen carrier materials in the related processes, CLC could be introduced into the process chain to lower the carbon footprint of these industries, e.g. for hematite or ilmenite a combination of CLC with a smelting process is proposed in a German patent [34]. A screening of Fe-based ores and by-products found that two samples, SSAB Röd and SSAB Brun, showed good and stable reactivity [26]. But these materials came in the form of very fine dust and the required production of particles would therefore increase the cost of the carriers. Iron oxide scale [26, 28] was also investigated as oxygen carriers but its reactivity was unstable and rather low.

The conversion of solid fuels in the fuel reactor consists of three steps - pyrolysis, gasification and combustion. Pyrolysis of the fuel takes place immediately after the fuel is introduced into the fuel reactor, producing volatiles and

char. The latter consists mainly of solid carbon and is, during the following gasification step, gasified to CO and H_2 by surrounding CO_2 or H_2O according to eq. 1 or eq. 2.

$$C + H_2O \Leftrightarrow CO + H_2 \quad (1)$$
$$C + CO_2 \Leftrightarrow 2CO \quad (2)$$

Finally, the gasification products and the volatiles reduce the oxygen carrier (M) yielding CO_2 and H_2O (eq. 3 and 4).

$$MO_x + H_2 \Leftrightarrow MO_{x-1} + H_2O \quad (3)$$
$$MO_x + CO \Leftrightarrow MO_{x-1} + CO_2 \quad (4)$$

According to the literature the gasification of the char (eq. 1 and 2) is the overall limiting step [35]. But, even if the reduction rate inherent to the oxygen carrier is of lower importance, when using solid fuels, it still has to be sufficiently fast to convert gasification products and volatiles before they leave the reactor. It is generally accepted that low cost oxygen carriers, as mentioned above, tend to have lower conversion rates. Low reactivity of the oxygen carrier directly leads to an increase of the required solids inventory [36]. This in turn leads to a larger pressure drop within the reactor and inevitably to increased power consumption to maintain the solid fluidization [37]. Therefore, it is worthwhile to search for oxygen carriers with high reactivity or for methods allowing increasing the reactivity of the existing low cost oxygen carriers.

This work aims to investigate the reactivity of four industrial by-products in a laboratory batch fluidized bed reactor using syngas (50% H_2 in CO) as fuel. Activated ilmenite was also tested as a reference material. The activation behaviour of the four materials, as well as their reactivity in the temperature range of 600 to 900ºC, has been determined.

Nomenclature

ω	mass based conversion of oxygen carrier
γ_{CO2}	CO_2 yield
m	mass of oxygen carrier
m_{ox}	mass of fully oxidized oxygen carrier
M_o	molar mass of oxygen
t	time
$\dot{n}$	molar flow

2. Experimental

2.1. Materials used

The oxygen carriers tested are iron-based industrial residues named bio_A (black iron oxide type A) , bio_C (black iron oxide type C) , LDst and AQS_US. All these materials are waste products or side stream from the steel production at SSAB in Oxelösund, Sweden. In addition a concentrate from a natural Norwegian rock ilmenite was used as reference. The materials have been gratefully provided by SSAB and Titania A/S, respectively. The composition of the SSAB materials after the removal of oxygen and organic materials is shown in Table 1. The composition of the Norwegian ilmenite can be found in previous work [23]. Prior to the experiments, all materials have been heat treated in a muffle oven at 850°C for nine hours. The heat treated samples have then been crushed and sieved to a particle size of 125-180 μm before being activated in the laboratory fluidized bed reactor.

Table 1. Element analysis of bioA, bioC, LDst and AQS_US.

wt. %	Fe	Mn	Ca	Si	Mg	K	Na	Al
bioA	74.3	0.55	0.011	0.04	0.002	0.002	0.002	0.03
bioC	73.0	0.35	0.11	0.62	0.01	0.01	0.01	0.1
LDst	17.1	2.3	30.7	4.6	5.4	0.08	0.04	0.58
AQS_US	23.9	2.0	22.7	6.4	4.9	0.1	0.13	2.53

2.2. Particle characterization

BET (Brunauer, Emmett and Teller) surface area and BJH (Barrett, Joyner and Halenda) pore volume have been obtained for all particles using a micromeritics Tristar 3000. The machine has a full-scale accuracy of ±0.5% and the data is presented in Table 2. Also in Table 2 is the crushing strength for all particles was determined using a Shimpo FGN-5. The value given is the average force in N from 30 individual measurements needed to crush a particle in the size fraction of 180-212 µm. In general, as can be seen in Table 2, the surface area increased by activation and that the crushing strength was similar for all oxygen carriers.

Table 2. BET surface area and crushing strength for oxygen carriers in this paper.

Sample	BET surface area (m^2/g)	Crushing strength (N)
bioC	0.14	1.3±0.5
bioC_acti	0.78	1.0±0.3
LDst	0.46	1.1±0.3
LDst_acti	0.75	1.0±0.2
AQS_US	0.93	1.0±0.2
Ilmenite_acti	0.36	1.3±0.3

2.3. Laboratory equipment

All experiments were carried out in a batch fluidized bed quartz glass reactor with an inner diameter of 22 mm and an overall length of 870 mm. A porous quartz plate in the reactor is used as gas distributor. The temperature is measured by CrAl/NiAl thermocouples located above the distributor. The fluidizing gas enters in the bottom of the reactor. The gas composition is controlled by mass flow regulators and magnetic valves. The water content in the off gas is condensed in a cooler before the concentrations of CO, CO_2 and O_2 are measured downstream in a gas analyzer (Rosemount NGA 2000).

The reactor is heated to the target temperature by an external electric furnace. During activation, a gas mixture consisting of 10% O_2 diluted with nitrogen is fed into the reactor with a total flow rate of 900 ml/min in the oxidation step and syngas (50% CO, 50% H_2) is introduced with the same flow rate in the reduction step. During testing of the oxygen carriers, syngas or CH_4 with a flow rate of 900 ml/min is fed into the reactor for testing of all materials in the reduction step while the oxidation gas is the same as that during activation. The oxidation and reduction steps are separated by inert periods where only N_2 is fed into the system for 180 s. The time for oxidation is 900 s and that of the reduction is 30 s for tests in the temperature range of 600-900°C. For all experiments 15 g of oxygen carrier were mixed with 10 g sand. The setup is presented in Fig 2 and has been used in previous work [2, 21, 23].

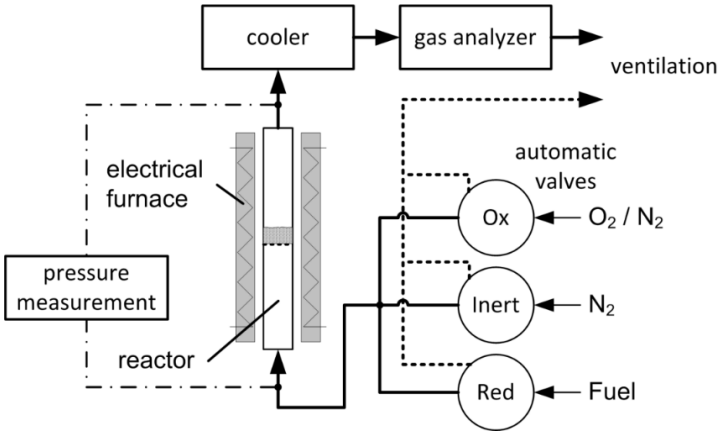

Fig. 2. Experimental set-up of the batch fluidized bed used in this work.

3. Data evaluation

The mass-based conversion of the oxygen carrier ω is calculated from the actual mass, m, and the oxidized mass, m_{ox}, according to eq. 5

$$\omega = \frac{m}{m_{ox}} \tag{5}$$

The oxygen carrier mass in its oxidized state, m_{ox}, was assumed to be equal to the raw mass of activated oxygen carrier. The oxygen carrier mass conversion ω is calculated according to eq. 6 for syngas and 7 for methane.

$$\omega(t_i) = 1 - \frac{M_O}{m_{ox}} \int_{t_0}^{t_i} (2\dot{n}_{CO_2}(t) + \dot{n}_{CO}(t) - \dot{n}_{H_2}(t))dt \tag{6}$$

$$\omega(t_i) = 1 - \frac{M_O}{m_{ox}} \int_{t_0}^{t_i} (4\dot{n}_{CO_2}(t) + 3\dot{n}_{CO}(t) - \dot{n}_{H_2}(t))dt \tag{7}$$

Here M_o is the molar mass of oxygen, t is time and $\dot{n}_x$ denotes the outgoing molar flow of CO_2, CO and H_2. The value for hydrogen is calculated by assuming that the water gas shift reaction has reached equilibrium [38]. The reaction rate of oxygen carriers is calculated according to eq.8.

$$\left.\frac{d\omega}{dt}\right|_i = \frac{\omega(t_i) - \omega(t_{i-1})}{t_i - t_{i-1}} \tag{8}$$

The CO_2 yield, γ_{CO2}, is the volume fraction of fully oxidized fuel, CO_2, divided by the sum of the volume fractions of carbon containing gases in the outlet stream, as given in eq. 9.

$$\gamma_{CO_2}(t_i) = \frac{\int_{t_{i-1}}^{t_i} \dot{n}_{CO_2}(t)dt}{\int_{t_{i-1}}^{t_i} (\dot{n}_{CO_2}(t) + \dot{n}_{CO}(t))dt} \quad (9)$$

The integral CO_2 yield, $\gamma_{CO2,int}$, is given according to previous publications [19, 23] in Eq. 10, describing the total amount of converted carbon during a given interval.

$$\gamma_{CO_2,\mathrm{int}}(t_i) = \frac{\int_{t_0}^{t_i} \dot{n}_{CO_2}(t)dt}{\int_{t_o}^{t_i} (\dot{n}_{CO_2}(t) + \dot{n}_{CO}(t))dt} \quad (10)$$

4. Results

Four low cost materials were investigated in the batch fluidized bed reactor. All the materials were first activated using redox cycles with syngas as fuel. Through activation, the reactivity of the oxygen carriers can be enhanced. This activation leads to morphological changes of the particles such as an increased porosity, the formation of cracks and the formation of a Fe-enriched outer shell [33]. Activation of ilmenite has previously been observed and described in detail [21, 23, 33]. Activation of the oxygen carriers was considered complete once the integral CO_2 yield remained constant from one cycle to the next, which indicates a stable reactivity. The integral CO_2 yield of bio_C, bio_A, LDst and AQS_US during the activation process is plotted in Fig. 3. For bio_A and bio_C, the activation required 5 redox cycles at 850°C and 7 redox cycles at 950°C using syngas as reducing gas and 10 vol.% O_2 in N_2 as oxidation gas. For LDst and AQS_US, the activation required 5 redox cycles at 850°C and 5 cycles at 950°C with the same reducing and oxidation condition. For ilmenite, the activation required 5 cycles at 850°C and 19 cycles at 950°C.

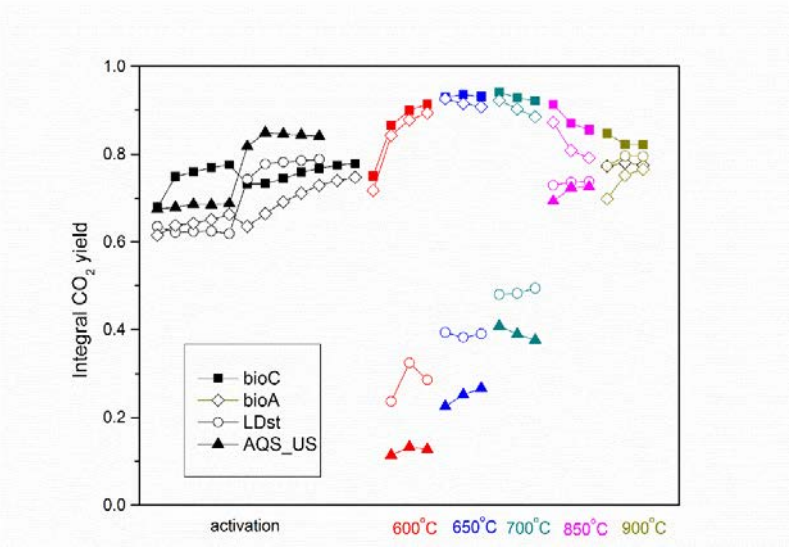

Fig. 3 Integral CO_2 yield obtained with syngas for bioC, bioA, LDst and AQS_US during activation and at different temperatures, every symbol represents one cycle.

For the low cost materials the integral CO_2 yield according to eq. 10 is presented for each reduction period as a function of the number of cycles in Fig.3. Bio_C and bio_A showed very similar behavior which is reasonable since

they have similar compositions, as shown in Table 1. Thus, in order to simplify the presentation, only Bio_C is presented in later figures.

The reduction rate was plotted in Fig.4 according to eq. 8 as a function of conversion ω. The CO_2 yield, defined in eq.9 is plotted in Fig. 5 as a function of conversion ω. The performance of activated ilmenite is shown in Fig. 4 and 5 as reference. In general, AQS_US and LDst show comparable performance to ilmenite while bio_C and bio_A perform better than ilmenite, especially at lower temperatures. For AQS_US and LDst, both the reduction rate and the integral CO_2 yield increase with temperature. The fraction of carbon converted is about 0.2 at 600°C and 0.8 at 900°C. However, for bio_C and bio_A, neither the reduction rate nor the integral CO_2 yield changes with temperature. This suggests that the reactivity of bio_A and bio_C is not limited by temperature at 600-900°C. Moreover, they perform slightly better at temperatures between 650°C and 700°C.

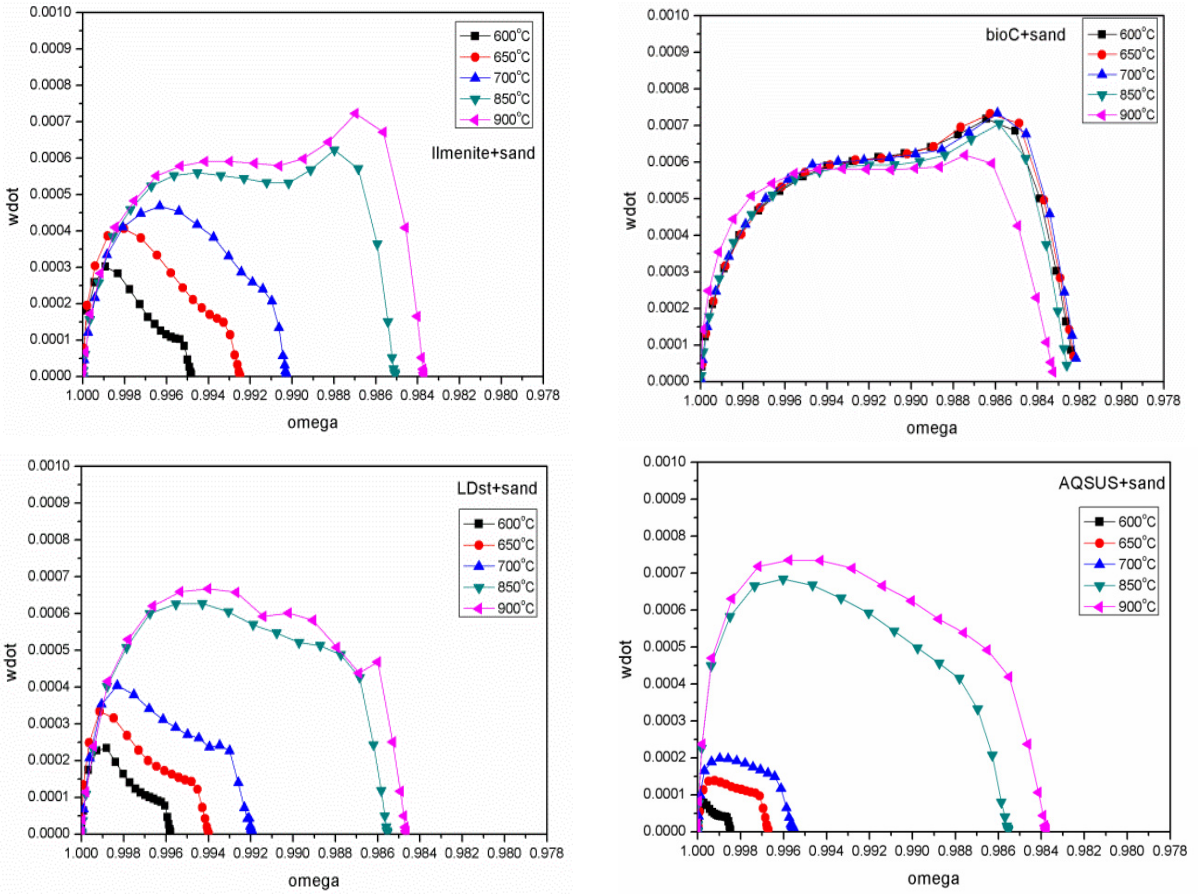

Fig. 4 Reaction rate (wdot) with syngas for activated ilmenite, bioC, LDst and AQS_US in the temperature range of 600-900°C as a function of oxygen carrier conversion ω (omega)

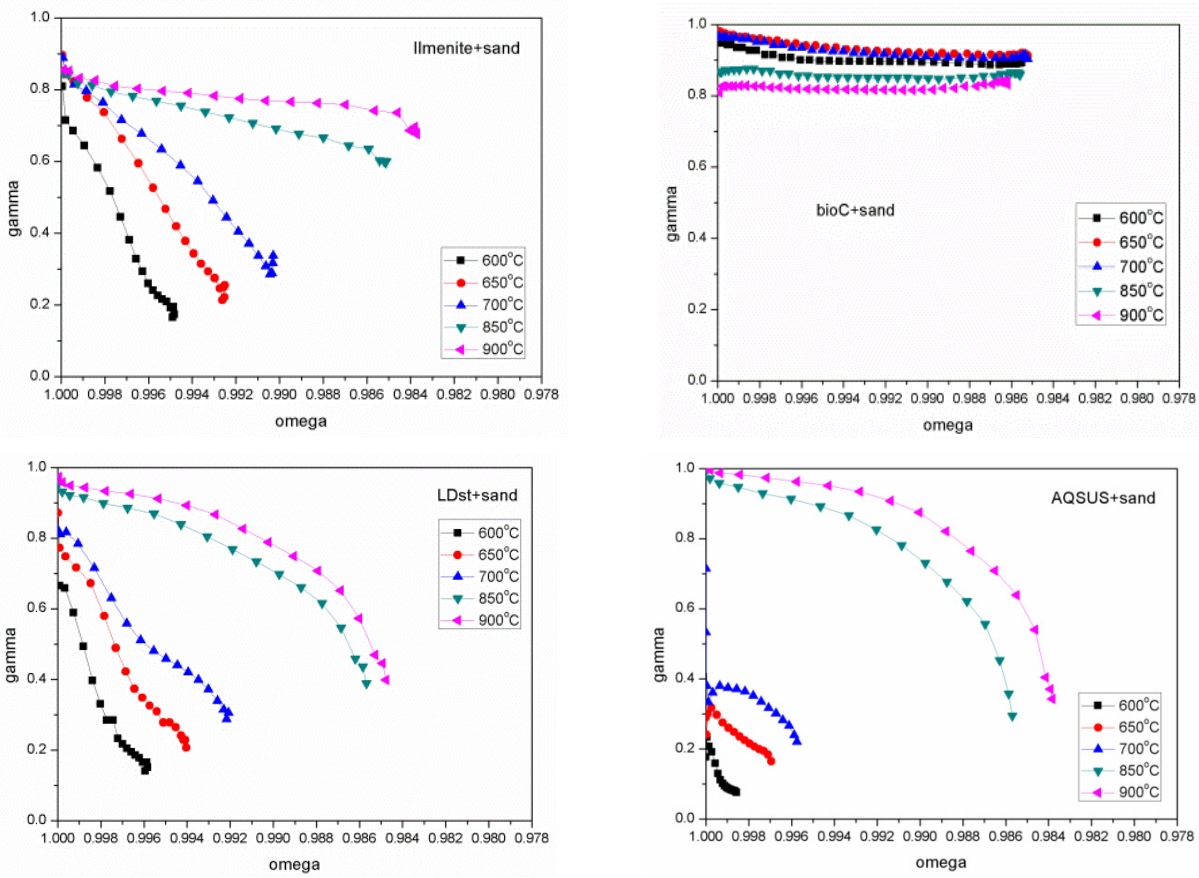

Fig. 5 CO_2 yield (gamma) with syngas for activated ilmenite, bioC, LDst and AQS_US in the temperature range of 600-900˚C as a function of oxygen carrier conversion

Since the tested carriers are waste products, they could be utilized as low-cost oxygen carriers. But still further tests in circulating units are needed. These materials would be practically suitable for use in the steel industry since significant amounts of these materials are already handled within the production process. Today a large fraction of these materials is used in construction or for landfills. If they could be used as oxygen carriers this would therefore increase the economic value of the material.

5. Conclusion

In the present study fluidized bed experiments have been performed on four low cost iron-based oxygen carriers (byproducts from the steel industry) with the widely used oxygen carrier ilmenite used as reference. The activation procedure for the oxygen carriers was determined and their performance in the temperature range of 600-900°C was investigated in a fluidized bed reactor. All the four byproducts (bio_A, bio_C, LDst and AQS_US) showed increased reactivity with increasing redox cycles.

Bio_A and bio_C showed higher reaction rate and integral CO_2 yield than ilmenite, especially in the temperature range of 600-700°C. LDst and AQS_US showed comparable performance to ilmenite with respect to reaction rate and integral CO_2 yield. As these waste products are very cheap, they could be promising as oxygen carriers candidates.

6. Acknowledgment

This work was supported by National Natural Science Foundation of China (51376105, 51061130535), the National Key Basic Research and Development Program (2011CB707301), Tsinghua University Initiative Scientific Research Program, and Program for New Century Excellent Talents in University (NCET-12-0304). Support was also given by Formas, the Swedish research Council for Environment, Agricultural Sciences and Spatial Planning.

References

[1] Ekström, C., et al. *Techno-Economic Evaluations and Benchmarking of Pre-combustion CO_2 Capture and Oxy-fuel Processes Developed in the European ENCAP Project*. in *the 9th International Conference on Greenhouse Gas Control Technologies (GHGT-9)*. 2008. Washington DC, USA.
[2] Schwebel, G.L., et al., *Apparent kinetics derived from fluidized bed experiments for Norwegian ilmenite as oxygen carrier.* Journal of Environmental Chemical Engineering, 2014. **2**(2): p. 1131-1141.
[3] Lewis, W.K., E.R. Gilliland, and W.A. Reed, *Reaction of methane with copper oxide in a fluidized bed.* Ind. Eng. Chem, 1949. **41**(6): p. 1227-1237.
[4] Lewis, W.K. and E.R. Gilliland, *Production of pure carbon dioxide*. 1954: USA.
[5] Knoche, K.F. and H. Richter, *Verbesserung der reversibilität von verbrennungsprozessen.* Brennstoff-Wärme-Kraft, 1968. **20**(5): p. 205-211.
[6] Richter, H.J. and K. K., *Reversibility of combustion processes.* ACS symposium series, 1983. **235**: p. 71-85.
[7] Ishida, M., D. Zheng, and T. Akehata, *Evaluation of a chemical-looping-combustion power-generation system by graphic exergy analysis.* Energy (Oxford, United Kingdom), 1987. **12**(2): p. 147-54.
[8] Ishida, M. and H. Jin, *A new advanced power-generation system using chemical-looping combustion.* Energy (Oxford, United Kingdom), 1994. **19**(4): p. 415-22.
[9] Adanez, J., et al., *Chemical Looping Combustion in a 10 kWth Prototype Using a CuO/Al_2O_3 Oxygen Carrier: Effect of Operating Conditions on Methane Combustion.* Industrial & Engineering Chemistry Research, 2006. **45**(17): p. 6075-6080.
[10] Jin, H. and M. Ishida, *Reactivity Study on Natural-Gas-Fueled Chemical-Looping Combustion by a Fixed-Bed Reactor.* Industrial & Engineering Chemistry Research, 2002. **41**(16): p. 4004-4007.
[11] Mattisson, T., et al., *Chemical-looping combustion using syngas as fuel.* International Journal of Greenhouse Gas Control, 2007. **1**(2).
[12] Jin, H. and M. Ishida, *A new type of coal gas fueled chemical-looping combustion.* Fuel, 2004. **83**(17-18): p. 2411-2417.
[13] Cao, Y., B. Casenas, and W.-P. Pan, *Investigation of Chemical Looping Combustion by Solid Fuels. 2. Redox Reaction Kinetics and Product Characterization with Coal, Biomass, and Solid Waste as Solid Fuels and CuO as an Oxygen Carrier.* Energy & Fuels, 2006. **20**(5): p. 1845-1854.
[14] Leion, H., T. Mattisson, and A. Lyngfelt, *Solid Fuels in Chemical-Looping Combustion.* International Journal of Greenhouse Gas Control, 2008. **2**: p. 180-193.
[15] Shen, L., et al., *Chemical-Looping Combustion of Biomass in a 10 kWth Reactor with Iron Oxide As an Oxygen Carrier.* Energy & Fuels, 2009. **23**(5): p. 2498–2505.
[16] Gu, H., et al., *Chemical Looping Combustion of Biomass/Coal with Natural Iron Ore as Oxygen Carrier in a Continuous Reactor.* Energy & Fuel, 2010. **25**: p. 446–455.
[17] Song, T., et al., *Evaluation of hematite oxygen carrier in chemical-looping combustion of coal.* Fuel, 2013. **104**: p. 244–252.
[18] Berguerand, N. and A. Lyngfelt, *Design and Operation of a 10 kWth Chemical-Looping Combustor for Solid Fuels – Testing with South African Coal.* Fuel, 2008. **87**: p. 2713–2726.
[19] Keller, M., et al., *Interaction of Mineral Matter of Coal with Oxygen Carriers in Chemical-Looping Combustion (CLC).* Chemical Engineering Research and Design, 2014. **92**(9): p. 1753-1770.
[20] Wen, Y., et al., *Experimental Study of Natural Cu Ore Particles as Oxygen Carriers in Chemical Looping with Oxygen Uncoupling (CLOU).* Energy & Fuel, 2012. **26**(6): p. 3919–3927.
[21] Leion, H., et al., *The use of ilmenite as an oxygen carrier in chemical-looping combustion.* Chemical Engineering Research and Design, 2008. **86**: p. 1017-1026.
[22] Arjmand, M., et al., *Use of Manganese Ore in Chemical-looping Combustion (CLC) - Effect on Steam Gasification.* International Journal of Greenhouse Gas Control, 2012. **8**: p. 56-60.
[23] Schwebel, G.L., et al., *Comparison of natural ilmenites as oxygen carriers in chemical-looping combustion and influence of the water gas shift reaction on the gas composition.* Chemical Engineering Research and Design, 2012. **90**(9): p. 1351-1360.
[24] Linderholm, C., et al., *Chemical-looping combustion of solid fuels – Operation in a 10 kW unit with two fuels, above-bed and in-bed fuel feed and two oxygen carriers, manganese ore and ilmenite.* Fuel, 2012. **102**: p. 808–822.
[25] Fossdal, A., et al., *Study of inexpensive oxygen carriers for chemical looping combustion.* International Journal of Greenhouse Gas Control, 2011. **5**(3): p. 483-488.
[26] Leion, H., T. Mattisson, and A. Lyngfelt, *Use of ores and industrial products as oxygen carriers in chemical-looping combustion.* Energy & Fuels, 2008. **21**(6): p. 2307–2315.
[27] Mendiara, T., et al., *Evaluation of the use of different coals in Chemical Looping Combustion using a bauxite waste as oxygen carrier.* Fuel, 2012. **106**: p. 814–826.
[28] Moldenhauer, P., M. Rydén, and A. Lyngfelt, *Testing of minerals and industrial by-products as oxygen carriers for chemical-looping combustion in a circulating fluidized-bed 300 W laboratory reactor.* Fuel, 2012. **93**: p. 351–363.
[29] Schwebel, G.L., et al., *Experimental comparison of two different ilmenites in fluidized bed and fixed bed chemical-looping combustion.*

Applied Energy, 2014. **113**: p. 1902–1908.
[30] Cuadrat, A., et al., *Ilmenite as oxygen carrier in a chemical looping combustion system with coal.* Energy Procedia, 2011. **4**: p. 362-369.
[31] Abad, A., et al., *Kinetics of redox reactions of ilmenite for chemical-looping combustion.* Chemical Engineering Science, 2011. **66**(4): p. 689–702.
[32] Ströhle, J., M. Orth, and B. Epple, *Design and operation of a 1MWth chemical looping plant.* Applied Energy 2014. **113**: p. 1490-1495.
[33] Adánez, J., et al., *Ilmenite Activation during Consecutive Redox Cycles in Chemical-Looping Combustion.* Energy & Fuels, 2010. **24**(2): p. 1402–1413.
[34] Schwebel, G.L., *DE 102009038052 B4*. 2009: Germany.
[35] Berguerand, N. and A. Lyngfelt, *The Use of Petroleum Coke as Fuel in a 10 kWth Chemical-Looping Combustor.* International Journal of Greenhouse Gas Control, 2008. **2**(2): p. 169-179.
[36] Lyngfelt, A., B. Leckner, and T. Mattisson, *A fluidized-bed combustion process with inherent CO2 separation; application of chemical-looping combustion.* Chemical Engineering Science, 2001. **56**(10): p. 3101-3113.
[37] Bao, J., Z.S. Li, and N.S. Cai, *Promoting the Reduction Reactivity of Ilmenite by Introducing Foreign Ions in Chemical Looping Combustion.* Industrial & Engineering Chemistry Research, 2013. **52**(18): p. 6119–6128.
[38] Cho, P., T. Mattisson, and A. Lyngfelt, *Carbon Formation on Nickel and Iron Oxide-Containing Oxygen Carriers for Chemical-Looping Combustion.* Industrial & Engineering Chemistry Research, 2005. **44**(4): p. 668-676.